# Hydrogen and halide co-adsorption on Pt(111) in an electrochemical environment: a computational perspective

Florian Gossenberger, Tanglaw Roman, Axel Groß

*Institute of Theoretical Chemistry, Ulm University, 89069 Ulm, Germany*

## Abstract

The adsorbate structures on electrode surfaces in an electrochemical environment are controlled by thermodynamic parameters such as temperature, concentration, pH and electrode potential. Knowledge of these structures is important as specifically-adsorbed ions on an electrode impact catalytic reactions that take place at the electrode-electrolyte interface. From a theoretical point of view, the equilibrium structures of adsorbates can be conveniently estimated using the concept of the computational hydrogen electrode. Here we extend this concept to determine equilibrium co-adsorption structures of halides with hydrogen on Pt(111) as a function of the corresponding electrochemical potentials. We find that hydrogen-halide co-adsorption is of a competitive character, which means that mainly dense-packed structures of either halides or hydrogens are stable on the surface, in good agreement with experiment.

## 1. Introduction

The adsorption of anions on metal electrodes is of particular interest in electrochemistry which is concerned with structures and processes at the interface between an ion and an electron conductor [1]. An electric double layer is formed at the electrochemical interface between the electrode and the electrolyte consisting of an electronic charge on the electrode and a corresponding ionic counter charge in the electrolyte. Anions such as halides often adsorb specifically [2], i.e., they form chemical bonds with the metal surface. These adsorbed anions change the work function of the electrode [3, 4], which is directly related to the electrode potential [5]. In addition, they affect the

chemical properties of electrodes by either directly participating in reactions at the surface or by modifying the electronic properties of the electrodes or by simply blocking adsorption and reaction sites [6, 7, 8, 9, 10, 11], or through cooperative effects, as in the underpotential deposition of metals [12].

In a previous paper we tackled the adsorption of halides on Pt(111) and Cu(111) [13] as a function of the electrode potential using the concept of the computational hydrogen electrode [14]. A similar work was also performed by McCrum *et al.* on halide adsorption at different Cu surfaces [15]. There is a rich literature on halide adsorption experiments on Pt(111) performed in ultra-high vacuum (UHV), air, or in electrochemical environments [2, 16, 17, 18, 19, 20, 21, 22, 23, 24, 25, 26, 27, 28, 29, 30, 31, 32, 33, 34, 35, 28, 29, 31, 36, 32, 34, 35]. Our previous study confirmed the experimentally-observed high coverage [2] of halides on metal electrodes [13]. Note that it is not distinguishable whether an adatom, which in general has a partial charge on the surface, was an ion or a neutral atom before adsorption. We therefore treat adsorbed halogen atoms and adsorbed halides as semantically identical; adsorbed hydrogen and adsorbed protons are likewise synonymous. However, any aqueous electrolyte also contains a certain concentration of protons, depending on the pH value. Especially platinum electrodes are covered by hydrogen at low electrode potentials [37, 38] because of the favorable hydrogen adsorption energy on Pt [39]. Here we extend the concept of the computational hydrogen electrode to describe the co-adsorption of halides and protons from first principles, similar to what has been done in heterogeneous oxidation catalysis using the related concept of ab initio thermodynamics [40]. This is in particular interesting as there might be some attractive electrostatic interaction between cations such as protons and anions such as halides adsorbed on a metal electrode.

Yet, to the best of our knowledge, the co-adsorption of halides and hydrogen on platinum has not yet been systematically studied from a theoretical perspective. The particular mechanisms underlying adsorbate-adsorbate interactions are still the subject of considerable debate [41]. Here we will derive phase diagrams of the stable co-adsorption structure of hydrogen with chlorine, bromine and iodine. Furthermore, for given concentrations of the ions, we will determine the surface coverage of hydrogen and halides as a function of the electrode potential and compare the results with those of corresponding experiments.

## 2. Theoretical Background and Computational Details

The aim of this paper is to link total energies of density functional calculations of a co-adsorbate system to thermodynamic values such as pH or electrode potential in order to derive phase diagrams of adsorbate structures. As a concrete system, a Pt(111) electrode covered by hydrogen and halides will be addressed, based on the concept of the computational hydrogen electrode [14].

Stable adsorption on surfaces is associated with a gain in Gibbs free energy of adsorption which is typically given per adsorbing atom or molecule. However, in this paper we will normalize the Gibbs energy to surface area $A_{\mathrm{S}}$ as this is the relevant entity to address the stability of surface phases. The most stable adsorbate structure in thermal equilibrium is therefore the structure with the lowest Gibbs free energy of adsorption $\Delta\gamma$,

$$\Delta\gamma = \frac{1}{A_{\mathrm{S}}}\left(G_{surf,ads} - G_{surf,0} - \sum_i n_i\mu_i\right) . \tag{1}$$

In this equation $G_{\mathrm{surf,ads}}$ and $G_{\mathrm{surf,0}}$ are the Gibbs free energies of the adsorbate-covered and the clean surface, $n_i$ is the number of adsorbed atoms of the type $i$ per surface area $A_{\mathrm{S}}$, and $\mu$ is the corresponding chemical potential of the ions in solution.

In the gas phase, the Gibbs free energy $G$ and the chemical potential $\mu$ depend on temperature and partial pressure of the molecules. The latter corresponds to the thermodynamic activity in solution. As far as solids are concerned, the temperature and pressure-dependent change in the Gibbs energy is rather small compared with the change in the Gibbs energy of liquids or gases. Therefore it is feasible to neglect this dependence and to consider it only for the ions in solution $\mu_i(T, p_i)$.

Furthermore, the chemical potential of charged particles is influenced significantly by the presence of the electrode potential. This is reflected in the so-called electrochemical potential $\tilde{\mu} = \mu + zeU$, where $z$ is an integer number for the charge of the particle, $e$ the elementary electric charge and $U$ the electrode potential. Note that we use the convention that the elementary electric charge is a negative number, in some publications a positive probe charge and an opposite sign are used. Adsorption energies on metal electrodes depend only very weakly on an applied electric field [14], therefore they hardly vary with electrode potential.

Hence we do not need to consider the dependence of $G_{\text{surf,ads}}$ and $G_{\text{surf,0}}$ on temperature, partial pressure or activity, and electrode potential, so that Eq. 1 can be written as

$$\Delta\gamma = \frac{1}{A_S}\Big(G_{\text{surf,ads}} - G_{\text{surf,0}} - \sum_i n_i \tilde{\mu}_i(T,p,U)\Big). \tag{2}$$

The Gibbs energy $G$ of both the adsorbate-covered and the clean surface can be derived from density functional theory (DFT) calculations. To be more precise, we can calculate the internal energy $U_{\text{int}}$ which is given as the total energy $E_{\text{tot}}$ in DFT. Furthermore, as the terms $TS$ as well as $pV$ are often quite small [42], we can approximate $G \approx U_{\text{int}}$.

To calculate the last term that corresponds to the electrochemical potential of the ions in solution, we use the concept of the computational hydrogen electrode [14]. It is based on the observation that under standard conditions (pH$= 0$, $T = 298$ K, $p = 1$ bar), defining the normal hydrogen electrode (NHE) there is an equilibrium between hydrogen molecules in the gas phase and solvated protons. Therefore the Gibbs free energy of the molecules in the gas phase $\mu_{\text{H}_2}$ is equal to the Gibbs free energy of the protons in aqueous solution plus the energy of an electron at the Fermi level in the metal $\tilde{\mu}_{\text{H}^+} + \tilde{\mu}_{\text{e}^-}$. Thus for this condition we do not need to compute the solvation energy of a proton in an aqueous solution but instead use the energy of the $H_2$ molecule in the gas phase as a reference which is much easier to derive from first principles. Furthermore, it is also known how the electrochemical potential depends on concentration and electrode potential. For these other thermodynamic conditions we just have to correct the NHE expression by an additional term $-eU_{\text{SHE}}$ for the electrode potential and by $-k_B T \ln(10)\text{pH}$ for the proton concentration.

$$\tilde{\mu}_{\text{H}^+} + \tilde{\mu}_{\text{e}^-} = \frac{1}{2}\mu_{\text{H}_2} - eU_{\text{SHE}} - k_B T \ln(10)\text{pH} . \tag{3}$$

Therefore it is possible to derive, starting from NHE conditions, the electrochemical potential at different electrode potentials and/or different concentrations. Hansen et al. pointed out that the same approach can be used for any redox couple $\frac{1}{2}A_2 + e^- \rightleftharpoons A^-$ [43]. In this way, this approach can be used to calculate the electrochemical potentials of any halides such as $\text{Cl}^-$, $\text{Br}^-$, and $\text{I}^-$ by

$$\tilde{\mu}_{\text{A}^-} - \tilde{\mu}_{\text{e}^-} = \frac{1}{2}\mu_{\text{A}_2} + e(U_{\text{SHE}} - U^0) + k_B T \ln(a_{\text{A}^-}), \tag{4}$$

4

where $U^0$ is the reduction potential of the corresponding halide which are listed in Tab. 1, and $a$ is the thermodynamic activity of the anion $A^-$. Since the reduction potential of hydrogen defines $0\,\mathrm{V}$ on the NHE scale, it does not appear in Eq. 3.

In the following, we will normalize the electrochemical potentials with respect to the total energy of the corresponding gas phase species. The electrochemical potentials $\Delta\tilde{\mu}$ of the proton $\mathrm{H}^+$ and the anions $\mathrm{A}^-$ are then given by

$$
\begin{aligned}
\Delta\tilde{\mu}_{\mathrm{H}^+}(T,p,U) &= \tilde{\mu}_{H^+}(T,p,U) + \tilde{\mu}_{\mathrm{e}^-} - \frac{1}{2}E_{\mathrm{H}_2} \\
&= -eU_{\mathrm{SHE}} - k_B T \ln(10)\mathrm{pH} \tag{5}
\end{aligned}
$$

and

$$
\begin{aligned}
\Delta\tilde{\mu}_{\mathrm{A}^-}(T,p,U) &= \tilde{\mu}_{A^-}(T,p,U) - \tilde{\mu}_{\mathrm{e}^-} - \frac{1}{2}E_{\mathrm{A}_2} \\
&= e(U_{\mathrm{SHE}} - U^0) + k_B T \ln(a_{\mathrm{A}^-}) \tag{6}
\end{aligned}
$$

which means that the internal total energies $\frac{1}{2}E_{\mathrm{H}_2}$ and $\frac{1}{2}E_{\mathrm{A}_2}$, respectively, at standard conditions have been taken out of the electrochemical potentials. When we then apply Eq. 2 to a co-adsorbed system of protons and halides, the Gibbs free energy of adsorption depends on the change of the chemical potentials of the protons $\Delta\tilde{\mu}_{H^+}(T,p,U)$ and the anions $\Delta\tilde{\mu}_{A^-}(T,p,U)$. Therefore the different co-adsorbed structures are planes in a three-dimensional diagram, where the $x$- and $y$-axes are the terms $\Delta\tilde{\mu}_{\mathrm{H}^+}(T,p,U)$ and $\Delta\tilde{\mu}_{\mathrm{A}^-}(T,p,U)$ and the $z$-axis is the Gibbs free energy of adsorption $\Delta\gamma$,

$$
\Delta\gamma(T,p,U) = \frac{1}{A_{\mathrm{S}}}\left(E_{\mathrm{ads}}^{\mathrm{tot}} - \sum_i n_i \Delta\tilde{\mu}_i(T,p,U)\right). \tag{7}
$$

The adsorption energy $E_{ads}^{tot}$ of $n_{\mathrm{H}}$ hydrogen atoms and $n_{\mathrm{A}}$ halide atoms per unit cell (with A=Cl, Br, or I) is evaluated according to

$$
E_{\mathrm{ads}}^{\mathrm{tot}} = E_{\mathrm{ads/slab}} - E_{\mathrm{slab}} - \frac{n_{\mathrm{H}}}{2}E_{\mathrm{H}_2} - \frac{n_{\mathrm{A}}}{2}E_{\mathrm{A}_2} \tag{8}
$$

| Redox couple | Reduction potential $U^0$ (V) |
|---|:---:|
| $\frac{1}{2}\mathrm{Cl}_2 + e^- \rightleftharpoons \mathrm{Cl}^-$ | 1.36 |
| $\frac{1}{2}\mathrm{Br}_2 + e^- \rightleftharpoons \mathrm{Br}^-$ | 1.09 |
| $\frac{1}{2}\mathrm{I}_2 + e^- \rightleftharpoons \mathrm{I}^-$ | 0.54 |

Table 1: Reduction potential of the halides considered in this work.

where $E_{\text{ads/slab}}$, $E_{\text{slab}}$, $E_{\text{H}_2}$ and $E_{\text{A}_2}$ are the total energies of the adsorbate-covered metal slab, the isolated metal slab, the H$_2$ molecule and the A$_2$ halogen molecule, respectively. Note that in the following we will neglect any dependence of $E_{\text{ads}}^{\text{tot}}$ on the thermodynamic conditions.

At given thermodynamic conditions, the stable adsorbate structure is given by the plane with the lowest Gibbs free energy of adsorption. It should be emphasized, that each area of stable equilibrium structures is derived from one DFT structure optimization. This makes the model computationally very attractive. However, the dependence of the adsorption energies on the presence of the electrolyte and on varying electrode potentials is entirely neglected. In principle, these dependencies can be included in the formalism of the computational hydrogen electrode. They are not taken into account here because, first, the adsorption energies of specifically adsorbed species is hardly modified by the presence of water [44], and second, on metals there is also little influence of any varying electric field on the adsorption energy [14], as already mentioned above.

Note also that the adsorption of hydroxide ions on the Pt(111) surface, which are always present in water, is not considered here as it is suppressed through the presence halides because their adsorption energy of 1.2 to 1.7 eV is larger than the OH-adsorption energy [45].

All DFT calculations in this paper were performed in a periodic supercell approach, using the density functional program VASP [46]. The exchange and correlation energy was taken into account by the functional of Perdew, Burke and Ernzerhof (PBE) [47]. For the electron-core interaction the projector augmented wave method was used [48, 49]. The electronic one-particle wave functions were expanded in a plane-wave basis set up to an energy cutoff of 500 eV.

The metal surface was represented by a slab of five atomic layers, the lower two layers were kept fixed at their bulk positions during the calculations and the upper three layers were completely relaxed. To model a variety of different surface structures and coverages, $(3 \times 3)$, c$(4 \times 2)$ and $(\sqrt{7} \times \sqrt{7}R19.1°)$ surface unit cells were considered containing between 9 and 12 metal atoms per layer. The integration over the first Brillouin zone was done using a gamma-centered $k$-point mesh with $7 \times 7 \times 1$ special $k$-points and a Methfessel-Paxton smearing of 0.1 eV [50].

| Halide | Structure | $\Theta$ (ML) | Refs. |
|--------|-----------|-----------|-------|
| Cl | $(3 \times 3)$ | 0.44 | [16, 17, 18, 19, 20, 21] |
| Cl | $c(4 \times 2)$ | 0.50 | [20] |
| Br | $(3 \times 3)$ | 0.44 | [22, 23, 24, 25, 26] |
| Br | $(3 \times 3\sqrt{3}/2)$ | 0.44 | [27] |
| Br | $(\sqrt{7} \times \sqrt{7}R19.1°)$ | 0.57 | [22] |
| I | $\sqrt{3} \times \sqrt{3}$ | 0.33 | [28, 29, 30, 31] |
| I | $(3 \times 3)$ | 0.44 | [22, 30, 32, 33, 34, 35] |
| I | $(\sqrt{7} \times \sqrt{7}R19.1°)$ | 0.43 | [22, 28, 29, 30, 31, 36, 32, 33, 34, 35] |

Table 2: Experimentally found surface structures of halides and co-adsorbed hydrogen on Pt(111).

## 3. Results and Discussion

### 3.1. Experimental data

Before discussing the results of our calculations, we first review the available experimental data on halide adsorption on Pt(111). Table 2 summarizes the results of some experimental studies of halide adsorption, which have been performed in UHV, air, or in electrochemical environments. Structures have been studied through both UHV and electrochemical in-situ techniques. Coverage/packing densities of adsorbed halides were deduced from Auger spectroscopic data in the vast majority of these studies. While several ordered structures of halides were found, a degree of uncertainty is always present in the assignment of adsorption sites.

As far as co-adsorbed systems are concerned, there are several studies that used HCl to introduce chlorine onto Pt(111) in UHV environments. High-resolution electron energy loss spectroscopy experiments [21] gave no hint of a Cl-H stretch for all HCl exposures used, indicating that HCl, upon adsorption, undergoes dissociation. Several studies [21, 51] have suggested that the adsorption of HCl molecules does not simply lead to a Cl-covered platinum (111) surface, but to a metal surface that is covered by both adsorbed atomic H and Cl. Low exposures (up to 0.25 L) of HCl undergo complete dissociation on Pt(111) at 90 K to form a disordered mixture of adsorbed H and adsorbed Cl. The simple kinetics and lack of an ordered LEED pattern in this regime suggests high mobility of the adatoms and/or adsorption into a well-mixed, disordered phase containing both adsorbed H and adsorbed Cl [21].

Wagner et al. [21] also found that exposures of 0.5 to 2 L HCl produce an ordered $(3 \times 3)$ phase in UHV. The fact that the same LEED pattern is seen for dosed HCl as for dosed $Cl_2$ shows that the Pt-Cl interaction is sufficiently strong to establish the Cl adsorption structure. It is suggested [21] that the co-adsorbed H is simply located in the areas unoccupied by Cl. The structure of the H atoms within the field of Cl atoms is unknown. One can question whether such structures even exist since H adatoms on pristine metal surfaces could be very mobile [52], but we also note that the presence of other adsorbed species can raise surface diffusion barriers [53], stabilizing co-adsorption. Hydrogen is believed to be co-adsorbed because the $H_2$ desorption following HCl dosing, though small, significantly exceeds the desorption area of background-derived hydrogen [21]. Adsorbed hydrogen leaves the surface through competing processes producing both $H_2$ and HCl. In contrast, in the study of Fukushima et al. [54] no hydrogen desorption was observed which led to the suggestion that atomic hydrogen and chloride exists in equal amounts on the $(3 \times 3)$ structures.

Chemisorbed iodide ions have been found to cause an overall decrease in the amount of adsorbed hydrogen on polycrystalline Pt surfaces [55]. There is practically no hydrogen adsorption on the surface covered by a monolayer of adsorbed iodide ions. This is consistent with the fact that on Pt(111), iodine forms a protective layer which prevents readsorption of contaminants while the clean sample cools to room temperature. Therefore it is possible to investigate iodine-covered Pt surfaces using STM in air [33, 34]. On the other hand, a monolayer of hydrogen was claimed to be adsorbed even when the surface is covered by the maximum amount of chloride and bromide anions [55]. From the observed increase in the second peak in the I-V curves, which corresponds to more weakly-bound H, it has been concluded that adsorbed chloride and bromide on polycrystalline Pt affect the energy distribution of adsorbed hydrogen (decreasing the bond energy, rather than the total amount adsorbed), while the total amount of the adsorbed H does not change [55]. This is supported by the finding that different reaction rates on Pt(100) were obtained with and without hydrogen transfer, attributed to interdiffusion of adsorbed hydrogen atoms in mixed chloride domains [56].

In electrochemical environments, it has been reported earlier [57] that the co-adsorption of chloride and hydrogen atoms has a synergistic character: the presence of hydrogen adatoms enhances chloride adsorption. This conclusion was however later shown to be a result of a surface that contained step defects [58, 51]. In these particular studies it was demonstrated that at
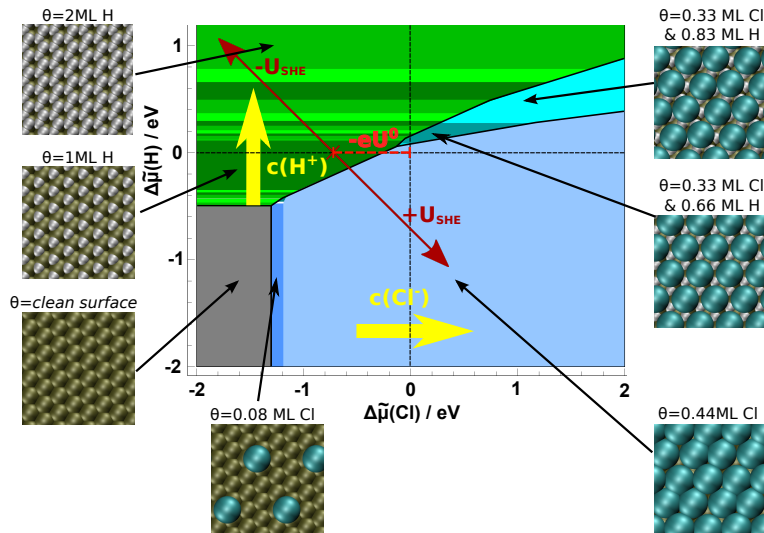
8

Figure 1: Stable phases of co-adsorbed chlorine and hydrogen on Pt(111) as a function of the electrochemical potential of hydrogen and chlorine. The green areas correspond to hydrogen-containing adsorbate structures, the blue areas to chlorine-containing structures and the cyan areas to mixed structures of both hydrogen and chlorine. The yellow arrows illustrate the effect of increasing the concentration of the species individually. The red double-arrow represents the effect of varying the electrode potential for fixed concentrations.

positive potentials, where Cl and H adsorption overlap, the adsorption has a competitive character. There is also evidence that the adatoms are not necessarily ionic at electrode-electrolyte interfaces, as the surface dipole is close to zero [51]. This is confirmed by DFT calculations which show that chlorine adsorption has an covalent character and that even a pure chlorine coverage does not cause an significant change in the surface dipole moment [59, 4].

### 3.2. Calculated phase diagrams for halide-hydrogen co-adsorption

In order to evaluate the phase diagram of stable halide-hydrogen co-adsorption phases, we first calculated the adsorption energies of 113 different structures within $(3 \times 3)$, $c(4 \times 2)$ and $(\sqrt{7} \times \sqrt{7}R19.1°)$ geometries. The corresponding adsorption energies $E_{ads}$ (Eq. 8) that are listed in the supplementary material were then used in Eq. 7 to construct the planes giving the Gibbs free energy of adsorption $\Delta\gamma$ as a function of the electrochemical
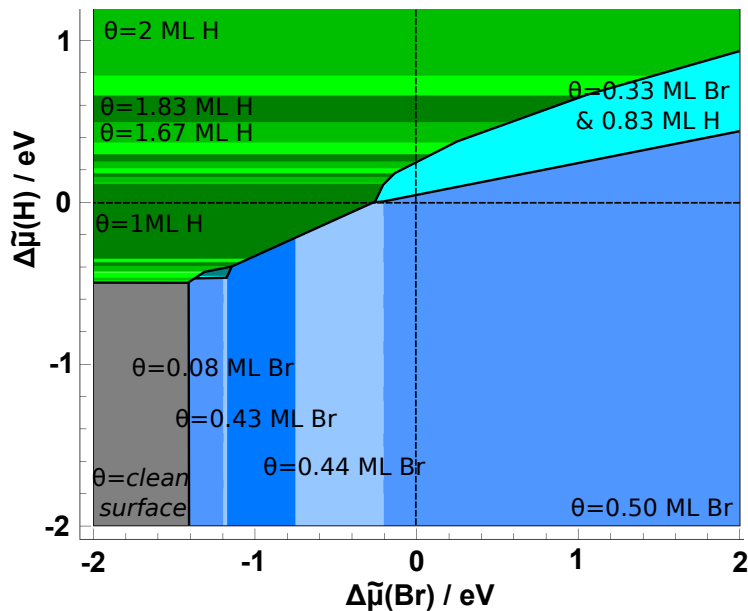
9

Figure 2: Stable phases of co-adsorbed bromine and hydrogen on Pt(111) as a function of the electrochemical potentials of hydrogen and bromine.

potentials $\Delta\tilde{\mu}_{A^-}$ and $\Delta\tilde{\mu}_{H^+}$.

In Fig. 1, the stable phases of co-adsorbed chlorine and hydrogen on Pt(111) as a function of the electrochemical potential of hydrogen and chlorine are plotted. The electrochemical potential depends on the concentration of the species and the electrode potentials. The yellow arrows illustrate how the electrochemical potential varies when the concentrations of the chlorine anions and the protons are varied separately, the red arrows indicate the effect of varying the electrode potential for fixed concentrations. The structures of some of the stable phases are illustrated in the pictures surrounding the phase diagram.

It is interesting to note that only a very small portion of the phase diagram corresponds to a true co-adsorption structure of hydrogen and chlorine. The phase diagram is dominated by areas that correspond either to pure hydrogen-adsorption or pure chlorine-adsorption phases or to the clean surface. As mentioned above, one would naively expect that there is some electrostatic attraction between adsorbed cations (protons) and anions (chloride). However, the simple picture of anionic adsorption of halides on metal
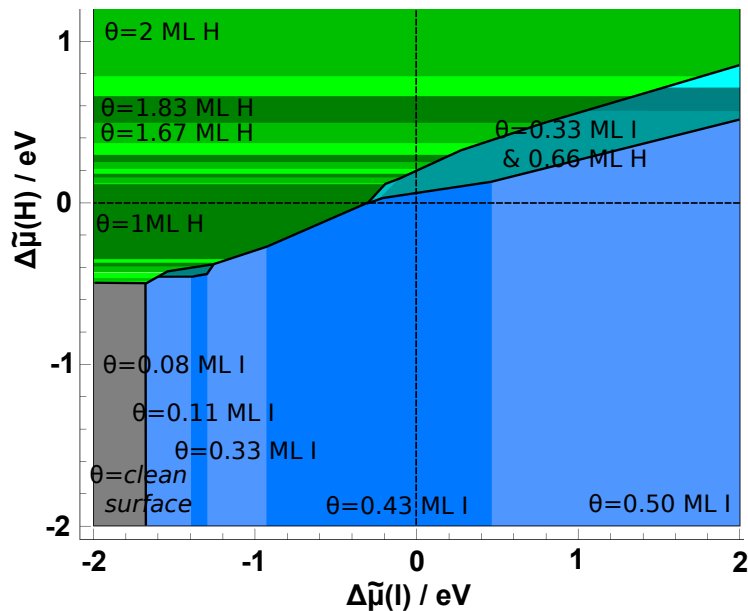
10

Figure 3: Stable phases of co-adsorbed iodine and hydrogen on Pt(111) as a function of the electrochemical potentials of hydrogen and iodine.

surfaces is obviously not correct. Experimentally, it is well-known that the adsorption of halogen atoms on metal surfaces leads to a reduction of the metal work function at low coverages [16, 24]. In principle, one would expect an increase in the work function upon the adsorption of negatively charged species. We have recently shown in a periodic DFT study that these anomalous work function changes upon halogen adsorption can be explained by the significant polarization of the adsorbed halogen atoms [3] which is particularly strong for iodine, but also present for bromine and chlorine [59, 4]. There is still a rather small net negative charge on the adsorbed halides, but the atomic polarization leads to a dipole moment at the surface that is opposite to what is expected for the adsorption of negatively charged species. Hydrogen adsorption on Pt(111) also leads to a small decrease in the work function [60], which means that there is a dipole-dipole repulsion between adsorbed hydrogen and halides. According to the calculated phase diagram, mixed structures may only exist for unusually high concentrations of both anions and protons.

We have furthermore also evaluated the phase diagram of stable phases of

11

hydrogen co-adsorbed with bromine (see Fig. 2) and iodine (Fig. 3). In principle, the phase diagrams of the three halides on Pt(111) look rather similar, indicating that the interactions of the adsorbed halides are comparable. For instance, our calculations yielded that the stabilities of the c($4 \times 2$) and the ($3 \times 3$) halides structures are rather similar.

Still, there are characteristic differences. In the chloride adsorption regime, Pt(111) is covered with the dense ($3 \times 3$) structure over a broad range of electrochemical potentials, whereas iodine shows five different stable patterns. Iodine is the only halide that exhibits a stable $\sqrt{3} \times \sqrt{3}$ adsorption structure at a coverage of $1/3$ ML as has also been observed in experiments [28, 29, 30, 31]. This $\sqrt{3} \times \sqrt{3}$ adsorption phase is particularly stable for iodine [13] compared to the higher coverage phases which might be caused by the fact that at higher coverages the significantly larger size of iodine compared to bromine and chlorine leads to a relatively larger repulsive interaction. Furthermore, iodine is the only halide for which the ($\sqrt{7} \times \sqrt{7}R19.1°$) structure is stable at a coverage of $3/7$ ML at larger electrochemical potentials, again in agreement with the experiment [22, 28, 29, 30, 31, 36, 32, 33, 34, 35].

We now focus on the regime in which hydrogen adsorption is stable. It is well known that under electrochemical conditions and low potentials, Pt(111) is covered by hydrogen [37, 38]. There is still some controversy between experiment and theory regarding the exact hydrogen equilibrium coverage. Whereas experiments indicate that at $0$ V relative to the normal hydrogen electrode (NHE) the hydrogen coverage should be about $0.66$ ML [38], DFT calculations rather yield a hydrogen coverage of $1$ ML [61, 39]. This is in fact also the case for our calculations here (for $\Delta\tilde{\mu}_{H^+} = 0 \ eV$). Still, there is a qualitative agreement that there is a significant hydrogen coverage. In the electrochemical literature, this strongly-adsorbed hydrogen is typically referred to as underpotential deposited (upd) hydrogen [1]. The presence of this hydrogen upd layer also has a significant influence on the water structure on Pt(111) at low potential as it weakens the metal-water interaction [62].

There is another, weakly-adsorbed hydrogen species that has been observed which is called overpotential deposited (opd) hydrogen [1]. The role of this opd hydrogen in the hydrogen electrocatalysis has just been intensively discussed from a theoretical point of view [63]. In particular, on transition metal surfaces, this weakly-bound species might play an important role in the hydrogen evolution reaction which is for example a crucial step in the electrolysis of water [64]. Our calculations confirm that at more positive chemical potentials of hydrogen much higher coverages become stable, reflected the
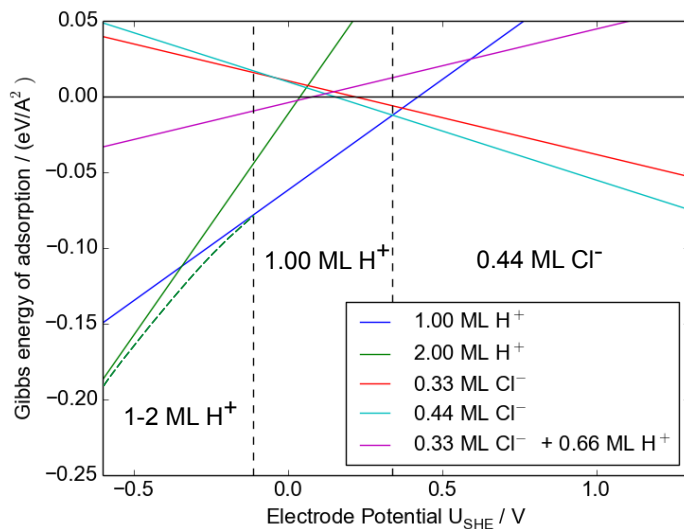
Figure 4: Calculated electrochemical equilibrium coverage of chlorine and hydrogen, co-adsorbed on a Pt(111) surface under standard conditions. At low electrode potentials, a variety of different stable hydrogen coverages between one and two ML exists (compare Fig. 1-3). To keep the figure comprehensive and clear, the Gibbs energy of these coverages are represented by a green, dashed line and exemplified by the 1 and 2 ML structures.

presence of opd hydrogen on Pt(111).

Note that the precise structure of ordered hydrogen phases on Pt(111) at different coverages is hard to identify by experimental techniques. This is due to two reasons: as hydrogen is a very weak scatterer, it cannot be easily detected by LEED, X-ray scattering, or STM. Furthermore, hydrogen can be very mobile – the hydrogen adatom's diffusion barrier on Pt(111) is in the order of only $0.06\,\mathrm{eV}$, and can even be effectively lower when delocalized nuclear quantum states of the hydrogen atom are considered [52, 65].

*3.3. Adsorbate structures as a function of electrode potential*

In electrochemical experiments, results are usually not reported as a function of electrochemical potentials, but rather as a function of the electrode potential for a given pH value and ion concentration. This information is all included in the phase diagrams Figs. 1-3. However, the explicit dependence of the stability of the considered adsorption phases on the electrode potential is not directly visible as the electrochemical potential scale has to be converted into an electrode potential scale. In fact, a variation of the

electrode potential with all other parameters kept unchanged corresponds to a diagonal cut through the two-dimensional phase diagrams, as illustrated in Fig. 1. The exact position of this diagonal depends on the concentrations.

In a previous paper, we addressed equilibrium adsorbate structures of halides on Cu(111) and Pt(111) as a function of the electrode potential, but without taking the effect of co-adsorbed hydrogen into account [13]. Here we present the stable structures of chlorine, bromine and iodine as a function of the electrode potential in Figs. 4-6, but this time with the taking into account the presence of protons in the electrolyte. Furthermore, we have considered more possible structures than done in Ref. [13].

The diagrams in Figs. 4-6 still correspond to a given combination of pH value and anion activity. For all three figures, we have assumed "standard conditions", i.e., we have assumed pH $= 0$ and $a_{A^-} = 1$. This means that the cuts corresponds to diagonals with slope $-1$ through the points $(\Delta\tilde{\mu}_{A^-}, \Delta\tilde{\mu}_{H^+}) = (-eU^0, 0)$ in the two-dimensional phase diagrams where $U^0$ is the corresponding reduction potential of the halides listed in Tab. 1. For these conditions, the free energy of adsorption can be expressed as

$$\Delta\gamma(U_{\text{SHE}}) = \frac{1}{A_{\text{S}}}\Big(E_{\text{ads}}^{\text{tot}} - n_{\text{A}}e(U_{\text{SHE}} - U^0) + n_{\text{H}}eU_{\text{SHE}}\Big). \qquad (9)$$

For the pure halide and the pure hydrogen adsorption phases this equation simplifies to [13]

$$\Delta\gamma_{A^-}(U_{\text{SHE}}) = \frac{n_{\text{A}}}{A_{\text{S}}}\Big(E_{\text{ads}}^{A^-} - e(U_{\text{SHE}} - U^0)\Big), \qquad (10)$$

$$\Delta\gamma_{H^+}(U_{\text{SHE}}) = \frac{n_H}{A_{\text{S}}}\Big(E_{\text{ads}}^{H^+} + eU_{\text{SHE}}\Big), \qquad (11)$$

where $E_{ads}^i$ is the adsorption energy per adatom, $E_{ads}^{tot}/n_i$. For other concentrations in the electrolyte, the reference point in the phase diagram needs to be shifted by $k_{\text{B}}T\ln a_{A^-}$ and/or by $k_{\text{B}}T\ln(10)$pH which at room temperature, e.g., corresponds to about $59\,\text{meV}$ if the activity is changed by one order of magnitude or if the pH is changed by one, respectively.

Again, the one-dimensional cuts through the phase diagrams for chlorine, bromine and iodine co-adsorption with hydrogen plotted in Figs. 4-6 look rather similar which is not too surprising considering the fact that the phase diagrams are rather similar. For all considered systems, no ordered co-adsorption phase becomes stable as a function of electrode potential. The calculated dependence of the free energy of adsorption of the purely
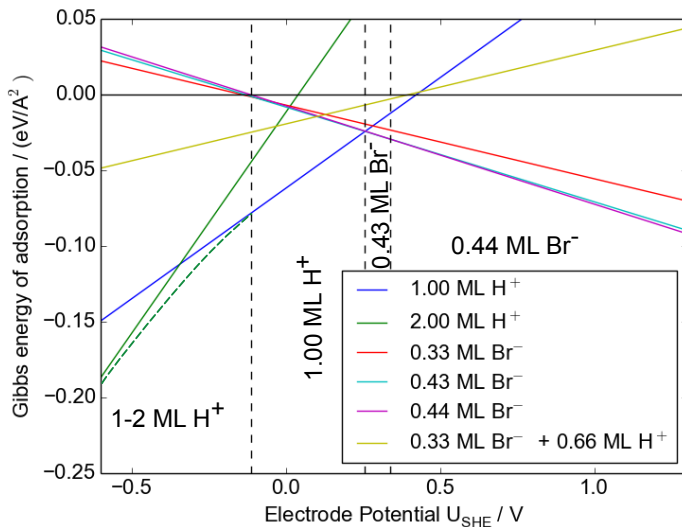
14

Figure 5: Calculated electrochemical equilibrium coverage of bromine and hydrogen, co-adsorbed on a Pt(111) surface under standard conditions. The hydrogen coverage phases at low electrode potentials are represented in the same way as in Fig. 4.

hydrogen-covered phases on the electrode potential agrees well with recent results obtained in DFT calculations with the aqueous electrolyte represented in a implicit solvent model [66]. There is a region at intermediate potentials in which both hydrogen adsorption and halide adsorption alone are thermodynamically stable, however, the adsorption has a competitive character, i.e., at lower potentials hydrogen adsorption is more stable, at higher potentials halide adsorption becomes more stable.

In the case of chloride and hydrogen adsorption on Pt(111) (see Fig. 4), chloride adsorption becomes thermodynamically stable at a potential of about $0.35\,\mathrm{V}$. Experimentally, measurements of the chloride and the hydrogen Gibbs excesses [58, 51] showed that in a narrow potential range $0.2 < E < 0.3\,\mathrm{V}$ (SHE) hydrogen and chloride can adsorb simultaneously on Pt(111). Still, the analysis of the electrosorption valencies implies that the adsorption of hydrogen and chloride has a competitive character [58, 51].

Note that the driving force for the adsorption of ions from solution is the gain in free energy per area upon adsorption. Hence an electrode surface might remain uncovered even when ions are present in solution as it rather corresponds to an open system in contact with a reservoir. This means
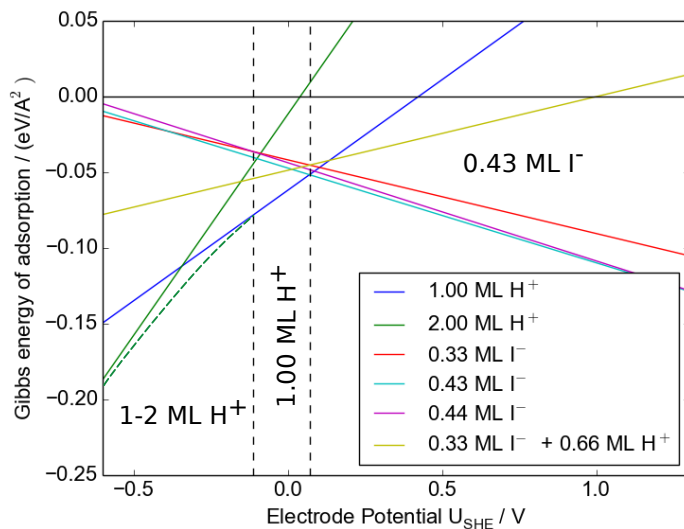
Figure 6: Calculated electrochemical equilibrium coverage of iodine and hydrogen, co-adsorbed on a Pt(111) surface under standard conditions. The hydrogen coverage phases at low electrode potentials are represented in the same way as in Fig. 4.

that in contrast to, e.g., solid solutions the concentration of ions on the surface is no parameter that can be modified continuously. Consequently, two distinct adsorbate phases can in principle only exist simultaneously on the surface if they are associated with exactly the same free energy of adsorption per area, which is realized at the potentials in Figs. 4-6 where the curve of the most favorable hydrogen adsorption phase crosses the curve of the most favorable halide adsorption phase. These considerations imply that thermodynamically, the competitive co-adsorption of two distinct adsorption phases over a range of potentials should not be possible if the dependence of their free energies of adsorption on the electrode potential is different. However, the experimental results concerning the co-adsorption of hydrogen and chloride were derived from cyclic voltammetry so that kinetic effects influence the results. Hence we believe that the experimental findings of hydrogen and chloride co-adsorption in a competitive manner over a narrow potential range are not at variance with our conclusions based on the surface phase diagrams.

As far as bromine (Fig. 5) and iodine adsorption (Fig. 6) on Pt(111) is concerned, we are not aware of any experimental studies that address the

co-adsorption with hydrogen in such detail. According to our calculations, these systems should also not exhibit any synergistic character, but rather be competitive, as far as hydrogen co-adsorption with bromine and iodine, respectively, is concerned. The onset of halide adsorption for bromine and iodine is shifted to lower electrode potentials compared to chlorine. This is caused by their stronger binding to Pt(111) [13], but also by their lower reduction potentials, as an analysis of Eq. 10 indicates.

Finally note that we extended the electrode potential range in Figs. 4-6 to negative values below -0.5 V. In principle, at negative potentials hydrogen evolution would take place which is, however, kinetically hindered. For that reason, it is also experimentally possible to scan to negative electrode potentials. Our calculations show that at potentials below -0.1 V hydrogen coverages larger than unity should become stable. This reflects the experimentally well-established observation of the occurrence of opd hydrogen.

## 4. Conclusions

The co-adsorption of hydrogen with the halides chlorine, bromine and iodine on Pt(111) surface has been studied by density functional theory calculations. Using a thermodynamic model based on the concept of the computational hydrogen electrode, the stable adsorbate phases as a function of the electrochemical potentials of hydrogen and halides have been derived. Because of the repulsive interaction between adsorbed hydrogen and halogen atoms, their adsorption is mainly competitive, which means that either purely hydrogen-covered phases or purely halogen-covered phases are stable.

By performing cuts through the two-dimensional phase diagram we have determined the stable adsorbate structures on Pt(111) as a function of the electrode potential. In the presence of chloride anions, according to our calculations there is small potential window in which hydrogen and chloride could in principle both adsorb individually on Pt(111). Still, their adsorption occurs in a competitive way which means that there is an electrode potential at which adsorbed hydrogen is replaced by chlorine upon increasing the electrode potential. As adsorbate phases correspond to an open system in contact with a reservoir, in thermal equilibrium no phase-separated co-existence of two immiscible adsorbate structures can occur except when their free energy of adsorption per area is exactly the same. Nevertheless, due to kinetic hindering there might still be a potential range over which the simultaneous

adsorption of two separate phases might be observed. These findings are in good agreement with corresponding experiments.

For bromine and iodine adsorption, the phase diagrams for the co-adsorption with hydrogen look very similar, only the replacement of hydrogen by these halides occurs at lower electrode potentials, caused by their stronger binding to Pt(111) and their lower reduction potentials. In general, our study confirms that the concept of the computational hydrogen electrode is rather useful for determining the structure of metal electrode/electrolyte interfaces.

## 5. Acknowledgments

[1] W. Schmickler and E. Santos, *Interfacial Electrochemistry*, Springer, Berlin, 2nd edition, 2010.

[2] O. M. Magnussen, Chem. Rev. **107** (2002) 679.

[3] T. Roman and A. Groß, Phys. Rev. Lett. **110** (2013) 156804.

[4] T. Roman, F. Gossenberger, K. Forster-Tonigold, and A. Groß, Phys. Chem. Chem. Phys. **16** (2014) 13630.

[5] S. Trasatti, Pure Appl. Chem. **58** (1986) 955.

[6] E. Spohr, G. Toth, and K. Heinzinger, Electrochim. Acta **41** (1996) 2131.

[7] C. M. Wei, A. Groß, and M. Scheffler, Phys. Rev. B **57** (1998) 15572.

[8] B. Hammer, Phys. Rev. B **63** (2001) 205423.

[9] M. Arenz, V. Stamenkovic, T. Schmidt, K. Wandelt, P. Ross, and N. Markovic, Surf. Sci. **523** (2003) 199.

[10] D. V. Tripkovic, D. Strmcnik, D. van der Vliet, V. Stamenkovic, and N. M. Markovic, Faraday Discuss. **140** (2009) 25.

[11] A. Groß, Surf. Sci. **608** (2013) 249.

[12] Z. Shi, S. Wu, and J. Lipkowski, Electrochim. Acta **40** (1995) 9.

[13] F. Gossenberger, T. Roman, and A. Groß, Surf. Sci. **631** (2015) 17.

[14] J. K. Nørskov, J. Rossmeisl, A. Logadottir, L. Lindqvist, J. R. Kitchin, T. Bligaard, and H. Jónsson, J. Phys. Chem. B **108** (2004) 17886.

[15] I. T. McCrum, S. A. Akhade, and M. J. Janik, Electrochim. Acta **173** (2015) 302.

[16] W. Erley, Surf. Sci. **94** (1980) 281.

[17] D. A. Stern, H. Baltruschat, M. Martinez, J. L. Stickney, D. Song, S. K. Lewis, D. G. Frank, and A. T. Hubbard, J. Electroanal. Chem. **217** (1987) 101.

[18] I. Villegas and M. J. Weaver, J. Phys. Chem. **100** (1996) 19502.

[19] R. Schennach and E. Bechtold, Surf. Sci. **380** (1997) 9.

[20] M. Song and M. Ito, Bull. Korean Chem. Soc. **22** (2001) 267.

[21] F. T. Wagner and T. E. Moylan, Surf. Sci. **216** (1989) 361.

[22] C. A. Lucas, N. M. Marković, and P. N. Ross, Phys. Rev. B **55** (1997) 7964.

[23] G. N. Salaita, D. A. Stern, F. Lu, H. Baltruschat, B. C. Schardt, J. L. Stickney, M. P. Soriaga, D. G. Frank, and A. T. Hubbard, Langmuir **2** (1986) 828.

[24] E. Bertel, K. Schwaha, and F. Netzer, Surf. Sci. **83** (1979) 439.

[25] S. Tanaka, S.-L. Yau, and K. Itaya, J. Electroanal. Chem. **396** (1995) 125.

[26] B. C. Schardt, J. L. Stickney, D. A. Stern, A. Wieckowski, D. C. Zapien, and A. T. Hubbard, Langmuir **3** (1987) 239.

[27] J. M. Orts, R. Gómez, J. M. Feliu, A. Aldaz, and J. Clavilier, J. Phys. Chem. **100** (1996) 2334.

[28] T. E. Felter and A. T. Hubbard, J. Electroanal. Chem. **100** (1979) 473.

[29] H. Farrell, Surf. Sci. **100** (1980) 613.

[30] F. Lu, G. N. Salaita, H. Baltruschat, and A. T. Hubbard, J. Electroanal. Chem. **222** (1987) 305.

[31] S. L. Yau, C. M. Vitus, and B. C. Schardt, J. Am. Chem. Soc. **112** (1990) 3677.

[32] J. L. Stickney, S. D. Rosasco, G. N. Salaita, and A. T. Hubbard, Langmuir **1** (1985) 66.

[33] B. C. Schardt, S.-L. Yau, and F. Rinaldi, Science **243** (1989) 1050.

[34] S. C. Chang, S. L. Yau, B. C. Schardt, and M. J. Weaver, J. Phys. Chem. **95** (1991) 4787.

[35] J. Inukai, Y. Osawa, M. Wakisaka, K. Sashikata, Y.-G. Kim, and K. Itaya, J. Phys. Chem. B **102** (1998) 3498.

[36] J. Stickney, S. Rosasco, and A. Hubbard, J. Electrochem. Soc. **131** (1984) 260.

[37] T. Schmidt, P. R. Jr., and N. Markovic, J. Electroanal. Chem. **524** (2002) 252.

[38] N. M. Marković and P. N. Ross Jr., Surf. Sci. Rep. **45** (2002) 117.

[39] S. Schnur and A. Groß, Catal. Today **165** (2011) 129.

[40] J. Rogal, K. Reuter, and M. Scheffler, Phys. Rev. B **75** (2007) 205433.

[41] S. T. Marshall and J. W. Medlin, Surf. Sci. Rep. **66** (2011) 173.

[42] K. Reuter and M. Scheffler, Phys. Rev. B **65** (2001) 035406.

[43] H. A. Hansen, I. C. Man, F. Studt, F. Abild-Pedersen, T. Bligaard, and J. Rossmeisl, Phys. Chem. Chem. Phys. **12** (2010) 283.

[44] A. Roudgar and A. Groß, Chem. Phys. Lett. **409** (2005) 157.

[45] N. Marković, H. Gasteiger, B. Grgur, and P. Ross, J. Electroanal. Chem. **467** (1999) 157 .

[46] G. Kresse and J. Furthmüller, Phys. Rev. B **54** (1996) 11169.

[47] J. P. Perdew, K. Burke, and M. Ernzerhof, Phys. Rev. Lett. **77** (1996) 3865.

[48] P. E. Blöchl, Phys. Rev. B **50** (1994) 17953.

[49] G. Kresse and D. Joubert, Phys. Rev. B **59** (1999) 1758.

[50] M. Methfessel and A. T. Paxton, Phys. Rev. B **40** (1989) 3616.

[51] N. Garcia-Araez, V. Climent, E. Herrero, J. M. Feliu, and J. Lipkowski, J. Electroanal. Chem. **582** (2005) 76.

[52] S. C. Badescu, P. Salo, T. Ala-Nissila, S. C. Ying, K. Jacobi, Y. Wang, K. Bedürftig, and G. Ertl, Phys. Rev. Lett. **88** (2002) 136101.

[53] T. Roman, H. Nakanishi, and H. Kasai, Phys. Chem. Chem. Phys. **10** (2008) 6052.

[54] T. Fukushima, M.-B. Song, and M. Ito, Surf. Sci. **464** (2000) 193.

[55] V. S. Bagotzky, Y. B. Vassilyev, J. Weber, and J. N. Pirtskhalava, J. Electroanal. Chem. **27** (1970) 31.

[56] B. Klötzer and E. Bechtold, Surf. Sci. **326** (1995) 218.

[57] N. Li and J. Lipkowski, J. Electroanal. Chem. **491** (2000) 95.

[58] N. Garcia-Araez, V. Climent, E. Herrero, J. Feliu, and J. Lipkowski, J. Electroanal. Chem. **576** (2005) 33.

[59] F. Gossenberger, T. Roman, K. Forster-Tonigold, and A. Groß, Beilstein J. of Nanotechnol. **5** (2014) 152.

[60] P. Ferrin, S. Kandoi, A. U. Nilekar, and M. Mavrikakis, Surf. Sci. **606** (2012) 679 .

[61] E. Skúlason, G. S. Karlberg, J. Rossmeisl, T. Bligaard, J. Greeley, H. Jónsson, and J. K. Nørskov,  Phys. Chem. Chem. Phys. **9** (2007) 3241.

[62] T. Roman and A. Groß, Catal. Today **202** (2013) 183.

[63] E. Santos, P. Hindelang, P. Quaino, E. N. Schulz, G. Soldano, and W. Schmickler, ChemPhysChem **12** (2011) 2274.

[64] R. de Levie, J. Electroanal. Chem. **476** (1999) 92.

[65] T. Roman, H. Nakanishi, W. Dino, and H. Kasai, e-Journal of Surface Science and Nanotechnology **4** (2006) 619.

[66] S. Sakong, M. Naderian, K. Mathew, R. G. Hennig, and A. Groß,  J. Chem. Phys. **142** (2015) 234107.